PLASTIC UPCYCLING

Chemical upcycling of polyethylene, polypropylene, and mixtures to high-value surfactants

Zhen Xu¹†, Nuwayo Eric Munyaneza¹†, Qikun Zhang², Mengqi Sun¹, Carlos Posada¹, Paul Venturo¹, Nicholas A. Rorrer^{3,4}, Joel Miscall^{3,4}, Bobby G. Sumpter^{5*}, Guoliang Liu^{1,6*}

Conversion of plastic wastes to fatty acids is an attractive means to supplement the sourcing of these high-value, high-volume chemicals. We report a method for transforming polyethylene (PE) and polypropylene (PP) at ~80% conversion to fatty acids with number-average molar masses of up to ~700 and 670 daltons, respectively. The process is applicable to municipal PE and PP wastes and their mixtures. Temperature-gradient thermolysis is the key to controllably degrading PE and PP into waxes and inhibiting the production of small molecules. The waxes are upcycled to fatty acids by oxidation over manganese stearate and subsequent processing. PP β -scission produces more olefin wax and yields higher acid-number fatty acids than does PE β -scission. We further convert the fatty acids to high-value, large-market-volume surfactants. Industrial-scale technoeconomic analysis suggests economic viability without the need for subsidies.

s the two most widely used commodity plastics, polyethylene (PE) (Table 1) and polypropylene (PP) contribute nearly 60% of the world's plastic production (~400 million tonnes), primarily for shortterm applications (1). The manufacturing of PE and PP is associated with the highest energy consumption among all plastics (1, 2) and contributes substantially to annual greenhouse gas emissions (2). Short-term use plastics quickly turn into waste and cause substantial pollution (3). To recycle PE and PP, the waste collection and sorting processes must be economically efficient to lower the cost (4), and the recycled products should ideally be high value and high volume to have a major impact on waste accumulation. Although PE and PP can be separated from heavier-than-water polymers such as polyvinyl chloride (PVC) and polyethylene terephthalate (PET) through a sink-float method that uses water as the medium (Fig. 1A), further separation of PE and PP is much more challenging because of their similar structures and densities. The two polymers are furthermore incompatible and cannot be blended unless expensive and sophisticated compatibilizers are used (5). Finding a generic and profitable method to recycle or upcycle both PE and PP while increasing their final product value over that of virgin plastics is thus imperative (3, 6-8).

¹Department of Chemistry, Virginia Tech, Blacksburg, VA 24061, USA. ²Department of Chemistry, Chemical Engineering and Materials Science, Ministry of Education Key Laboratory of Molecular and Nano Probes, Shandong Normal University, Shandong 250014, PR China. ³Renewable Resources and Enabling Sciences Center, National Renewable Energy Laboratory, Golden, CO 80401, USA. ⁴BOTTLE Consortium, Golden, CO 80401, USA. ⁵Center for Nanophase Materials Sciences, Oak Ridge National Laboratory, Oak Ridge, TN 37831, USA. ⁵Department of Chemical Engineering, Department of Materials Science and Engineering, Macromolecules Innovation Institute, Virginia Tech, Blacksburg, VA 24061, USA. **Corresponding author. Email: gliul@vt.edu (G.L.); sumpterbg@ornl.gov (B.G.S.) †These authors contributed equally to this work.

and is envisioned as a solution that converts postconsumer wastes into high-value chemicals, e.g., the conversion of polystyrene (PS) into aryl carbonyls and aryl alkyls (9-11). Chemical upcycling of PP and PE, however, is difficult because of the high ceiling temperatures involved (12). Moreover, the lack of heteroatomassociated weak links within the polymer chains (e.g., esters in PET) provides no selective chainscission sites. Product control is thus exceptionally challenging. Recently, chemical reactions that use iridium- (13) and platinum-based catalysts (14) and ionic liquids (15) generated fuels and improved selectivity toward aryl moieties in the upcycling of PE. On a laboratory scale, PE can also be converted to propylene by dehydrogenation and tandem isomerizing ethenolysis (16, 17). Considering the technoeconomic potential for increased product value and generalizability to both PE and PP, the conversion of polyolefins to high-value fatty acids or ionic surfactants is appealing because PE and PP are aliphatic by nature. In addition, surfactant products have huge market demands (i.e., comparable to plastics) and high economic values (i.e., higher than fuels, waxes, and regular aromatic compounds) (table S1). Moreover, surfactant products such as soaps are made from fatty acids of varying chain lengths and are often blended with ketones and aldehydes to soften the product and modulate fragrance release (18), diminishing the need to remove ketone and aldehyde by-products in the upcycling process of PE and PP. Biodegradation converts PE to fatty acids by means of microbial strains, but the fermentation period is too long (>10 days) to be practically deployable in the chemical industry (19). Chemically, the Novoloop method and hydrothermal reactions with strong oxidants quickly degrade PE but require harsh reaction conditions, such as strong nitric acid and high pressure (20, 21). Most re-

Chemical upcycling increases product value

cently, metallization of PE over Zr and aluminum has afforded products with trollable average carbon-chain lengths, and the catalysts must operate under O_2 -, CO_2 -, and H_2O -free conditions (22). Therefore, time- and material-efficient methods that use noncorrosive chemicals, atmospheric pressure, and airtolerant reaction conditions are highly sought to efficiently transform both PE and PP into large-market-volume fatty acids, preferably without the need for additional sorting and separation but with high selectivity and conversion.

Here we report a gradient-temperature thermolysis method that can selectively break PE, PP, and their mixtures into waxes under atmospheric pressure (Fig. 1, A and B). The key is that the temperature gradient prevents violent pyrolysis reactions, quenches vaporized waxes, and inhibits complete degradation to small molecules (Fig. 1C and figs. S1 and S2; see discussion in supplementary materials). PE- and PP-derived waxes are subsequently transformed into fatty acids with high acid numbers (ANs) and number-average molar masses of up to ~700 and 670 Da, respectively (Fig. 1D and tables S2 to S4). Through subsequent saponification, we obtain an ionic surfactant product that contains salts of fatty acids. Simply mixing with additives (e.g., fragrances) can produce commercial products, such as soap bars and liquid detergents (examples in Fig. 1A), which have higher market values than typical chemical products such as fuels and alkylaromatics (11, 14).

Polyethylene conversion to fatty acids

Initially, pulverized lab-grade PE (~500 mg; $M_{\rm w}$, 97 kDa; polydispersity $\theta = 2$) was loaded into a custom-designed quartz reactor (Fig. 1A and fig. S1) and purged with gases of controlled compositions (N2, 10 vol % O2 in N2, or air). The degradation was initiated by heating the bottom of the reactor to ~360°C stepwise with a step size of ~100°C per 5 min. Polymer smokes (fig. S2) appeared, indicating the vaporization of fragmented polyolefins or waxes. The waxes were condensed in the cold part of the reactor, preventing further fragmentation to shorter hydrocarbons. The wax yields from PE degradation in N_2 (PE- N_2 -wax), 10 vol % O_2 (PE-O-wax), or air (PE-air-wax) were 86, 79, and 55 wt % (Fig. 2A and table S2, experiments 1 to 3, 7 to 9, and 13), respectively. In a control experiment under N2 without a temperature gradient, the products were mostly short-chain hydrocarbons of C8 and below (Fig. 1C).

Gas chromatography–mass spectrometry (GC-MS) was used to characterize the wax composition (Fig. 2B), showing mainly solid waxes with minor fractions of light hydrocarbons (~10 wt % of C8 and below, fig. S3). Each primary peak could be resolved into a doublet of alkene and alkane with the same carbon number (figs. S4 and S5), similarly to degradation in flow reactors (23). In the presence of O_2 ,

Xu et al., Science **381**, 666-671 (2023) 11 August 2023 **1 of 6**

PE-O-wax and PE-air-wax exhibited GC-MS peaks and molecular ion signals similar to those of PE-N2-wax. PE-O-wax and PE-air-wax showed stronger intensities at shorter elution times than PE- N_2 -wax (Fig. 2B), indicating more short hydrocarbons and lower average molecular weights as a result of accelerated degradation by oxygen radicals (24). The PE-air-wax vield was too low (~55%), albeit higher than those in the literature (25, 26), to be practically useful for generating hydrocarbons suitable for downstream production of surfactants (Fig. 2A); therefore, no further characterization of PE-air-wax was conducted. High-temperature gel permeation chromatography (HT-GPC) confirmed the degradation of polymers (fig. S6). Because HT-GPC cannot resolve the exact molecular weights in this range, and because GC cannot detect low-volatility heavy hydrocarbons (>C40) (27), atmospheric pressure chemical ionization mass spectrometry (APCI-MS) was used to analyze the full composition. The spectra of PE-N2-wax and PE-O-wax showed waxes of mass/charge ratio (m/z) centered at

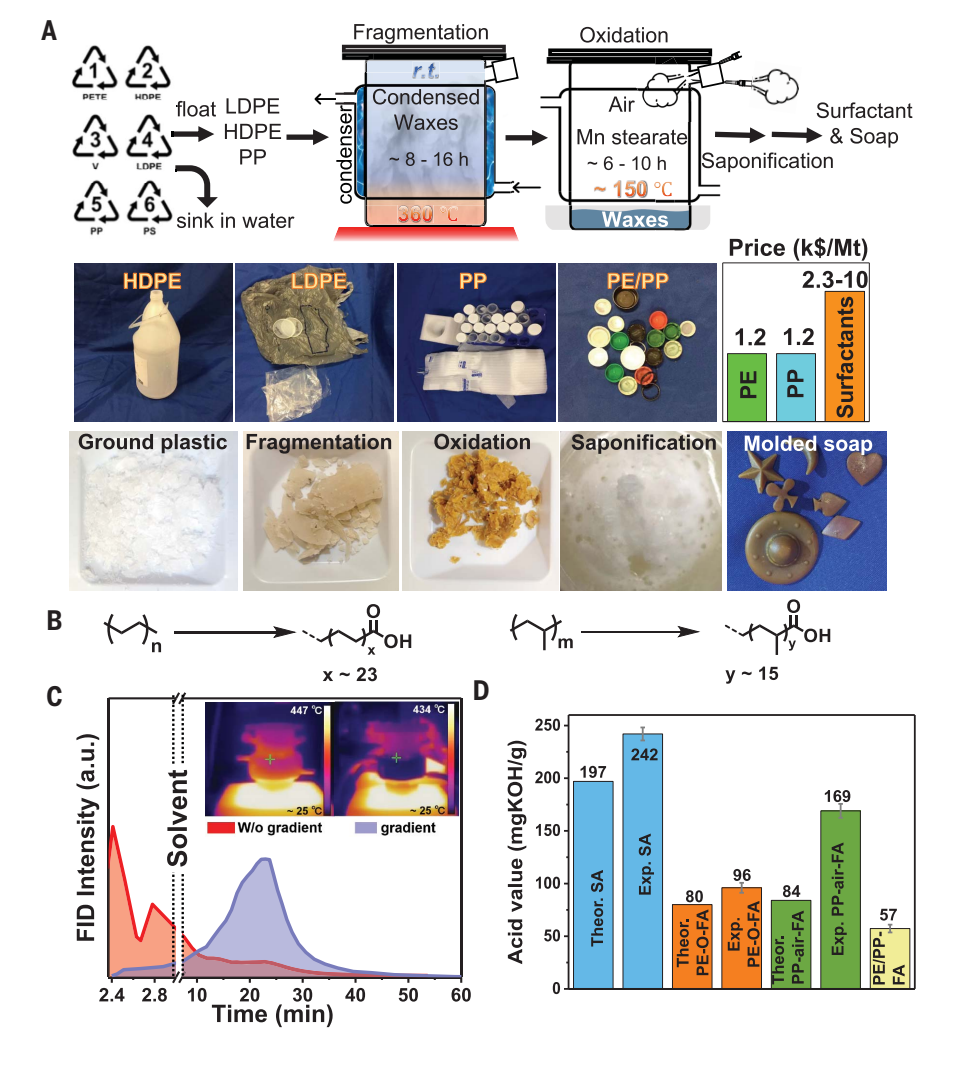
~630 and 540 (fig. S6 and table S3), corresponding to a carbon number of ~45 and 42, respectively. Despite m/z ranges of 300 to 1000 for PE-N2-wax and 200 to 900 for PE-O-wax (fig. S6C), the polydispersities were relatively small (<1.1, table S3). The PE-N2-wax and PE-O-wax were further characterized by nuclear magnetic resonance (NMR) spectroscopy through heteronuclear multiple bond correlation (HMBC) and heteronuclear single quantum correlation (HSQC) experiments (Fig. 2C and figs. S7 and S8) to investigate the waxes' structures. NMR confirmed the presence of unsaturated carbon in both PE-N₂-wax and PE-O-wax, showing primarily 2-propenyl at the chain end (¹H NMR δ 5.0 and 5.8, 13 C NMR δ 114 and 138) and minor internal alkenes (13 C NMR δ 123 to 131). The presence of O2 partially oxidized PE-O-wax and produced ketones, aldehydes, and esters (fig. S8).

Upcycling of the waxes was conducted over Mn compounds for 10 hours in an airflow at 150°C. Although inorganic MnO₂ and KMnO₄ have shown effectiveness in paraffin oxidation (28), they were ineffective in oxidizing PE-derived

wax, probably because of low miscibility, showing no appreciable carbonyl signals after 24 hours (fig. S9). By contrast, Mn stearate catalyzed the oxidization of PE-derived wax much faster owing to the better dispersion of the catalyst in the organic media (29, 30). The oxidation rates of PE-N2-wax or PE-O-wax were similar over Mn stearate (5 wt % loading) under a constant air flow, as shown by the similar slopes of carbonyl index (CI) changes as a function of time. PE-O-wax showed a higher final CI because of the higher initial value than did PE-N2-wax. We conclude on the basis of HMBC analysis that the oxidation of PE-O-wax over Mn stearate intensified the carbonyl concentration in the first 6 hours (figs. S9 and S10. 13 C NMR δ 160 to 206), producing primarily aldehydes and minor esters, ketones, and carboxylic acids. The oxidation likely occurred by means of a radical addition mechanism (31, 32), possibly through epoxy intermediate rearrangement to aldehydes and ketones (33). The presence of aldehyde was confirmed by NMR-HMBC, whereas epoxy signals were too weak to

Fig. 1. Upcycling of PE and PP to fatty acids in a temperature-gradient reactor.

(A) Schematic process flow of separation and upcycling of commercial polyolefins, including high-density PE (HDPE), lowdensity PE (LDPE), and PP to soap products performed using a custom-designed gradient thermal reactor. The temperaturegradient reactor has a hot and cold zone. preventing complete thermolysis of PE and PP to small molecules, and is key to controlling the chain length of fragmented products. Photographs show representative PE and PP wastes used in this study (HDPE container, grocery bags, sandwich bags. bottle caps, PP centrifuge tubes, and PP foam), as well as the products of intermediate waxes, fatty acids, surfactant solution, and soap molded into various shapes. The market price per metric ton of common surfactant products is almost double that of virgin plastics (table S1). (B) Reaction schemes of upcycling PE and PP to fatty acids. (C) Representative product distributions after PE degradation in the reactor with and without temperature gradient. The distribution and intensity were measured with GC. Signals from 3 to 7 min overlapped with the toluene solvent and thus were not shown for clarity. (Inset) Infrared thermal image of the reactor with and without temperature gradient. (D) AN of resulting fatty acids compared with that of stearic acid (SA, C18) and theoretical values of fatty acids with average carbon numbers of C47 for PE and C45 for PP. The error bars are the standard deviation of at least three replicates.



Xu et al., Science 381, 666-671 (2023) 11 August 2023 2 of 6

be confirmed. The dominance of aldehyde intermediates agreed well with the simulation results. Because aldehydes were susceptible to further oxidation, they were converted to acids (Fig. 2D, 13 C NMR δ 180) in the latter 2 hours of oxidation and subsequent saponification in 0.1 M aqueous KOH. The saponification hydrolyzed minor fatty esters and increased the amount of fatty acids; it also helped remove undesired short-chain acids (e.g., acetic acids). Hydroxyl signals were too weak to confirm the presence of alcohols in the product. The saponified solution was neutralized with HCl, crashing out fatty acid (PE-O-FA). After washing and drying under a vacuum, PE-O-FA was characterized by HMBC, showing primarily carboxylic acids and minor ketones. Aldehydes were no longer detectable (fig. S11). The carboxyl in the fatty acid correlated with two types of protons (Fig. 2D, ¹H NMR δ 2.0 and 1.5), potentially indicating a carboxyethyl end group. The AN of the PE-O-FA was determined by titration, giving an ordinary AN of 96 mg KOH/g (Fig. 1D and table S4) that slightly exceeded the theoretical value of ~80 mg KOH/g for a 700 g/ mol monocarboxylic acid (C47).

Extension to polypropylene and mixtures

After successfully converting PE to fatty acids, the process was applied to pulverized lab-grade PP (500 mg; $M_{\rm w}$, 158 kDa; Φ =4) under reaction conditions similar to those used for PE (N_2 , 10 vol % O₂ in N₂, and air). Degradation products in N₂ (PP-N₂-wax), 10 vol % O₂ (PP-O-wax), and air (PP-air-wax) showed total wax yields of 90, 85, and 87 wt %, respectively (Fig. 3A and table S2, experiments 4 to 6, 10 to 12, and 14), with a small amount of coke and gaseous products (fig. S12). The m/z ranges were 170 to 950 (centered at 560) for PP-N2-wax and 150 to 700 (centered at 450) for PP-air-wax (fig. S6C), and the molecular weight polydispersities were relatively small (table S3). Unlike that for PE, the PP wax yield remained high in the air, eliminating the need for controlled gases in the process and making the method more economically attractive. Therefore, the degradation of PP in 10 vol % O2 was not investigated further. GC-MS analysis of PP-N2-wax showed broad multimodal distributions of primarily alkene products in GC-MS (fig. S13). The carbon numbers of alkenes were mostly multiples of 3 (or 3n in the range of C9 to C36), and those of the rest of alkanes, alkenes, and dienes were mainly 3n+1. This distribution suggested that the primary degradation mechanism could be chain scission on the PP backbone because each PP repeating unit has three carbons (which is in agreement with our simulations below). With air present, the chromatogram of PP-air-wax became crowded and hard to analyze (fig. S6A). PP-N2-wax and PP-air-wax were characterized by APCI-MS (fig. S6, B and C), and the latter showed a slightly higher proportion of short

Table	1 1	Abbrevia	4:
1 an	ie i.	Annrevia	TIONS.

Full name	Abbreviatio
Chemicals	
Polyethylene	PE
Polypropylene	PP
Polyvinyl chloride	PVC, or V
Polyethylene terephthalate	PET
High-density PE	HDPE
Low-density PE	LDPE
Stearic acid	SA
Wax yielded from PE degradation in $ m N_2$	PE-N ₂ -wax
Wax yielded from PE degradation in 10 vol % 0 ₂	PE-O-wax
Wax yielded from PE degradation in air	PE-air-wax
PE-O-wax derived fatty acid	PE-O-FA
Wax yielded from PP degradation in N ₂	PP-N ₂ -wax
Wax yielded from PP degradation in 10 vol % O ₂	PP-O-wax
Wax yielded from PP degradation in air	PP-air-wax
PP-air-wax derived fatty acid	PP-air-FA
Instrumentation and methods	
Gas chromatography	GC
Gas chromatography-mass spectrometry	GC-MS
High-temperature gel permeation chromatography	HT-GPC
Atmospheric pressure chemical ionization mass spectrometry	APCI-MS
Nuclear magnetic resonance spectroscopy	NMR
Heteronuclear multiple bond correlation	HMBC
Heteronuclear single quantum correlation	HSQC
Proton NMR	¹H NMR
Ouantitative NMR	q-NMR
Flame ionization detector	FID
Mass selective detector	MSD
Density functional–based tight-binding	DFTB
ab initio molecular dynamics	AIMD
Fourier transform infrared spectroscopy	FTIR
Thermogravimetric analysis	TGA
Herriogravinietric arialysis	IGA
Parameters	
Number-average molar mass	M _n
Weight-average molar mass	$M_{ m w}$
Polydispersity	Đ
Carbonyl index	Cl
Acid number	AN
Activation energy	Ea
Pre-exponential factor	A
Selectivity of thermolysis (T) or upcycling (U)	s _T or s _U
Yield of thermolysis (T) or upcycling (U)	α_T or α_U
Concentration of alkenyl groups	$c_{c=c}$
Concentration of total waxes	C _{wax}
Concentration (mmol/g) of acid group in fatty acids	C _{acid}
Concentrations (mmol/g) of alkenyl groups in fatty acids	$C_{c=c,FA}$

hydrocarbons because of air-induced oxidation, which is similar to the finding in a previous report. (34) As with the PE degradation product, PP-N₂-wax and PP-air-wax were primarily composed of terminal alkenes with minor internal alkenes (Fig. 3B and figs. S14 and S15). The primary form of the terminal alkene was possibly 2-methyl-2-propenyl, as suggested by the correlations in the HMBC and HSQC. Additionally,

some minor forms of alkenes were detected in the 13 C NMR spectra and could be ascribed to internal alkenyl structures (fig. S14A). PP-airwax contained ketones, aldehydes, and esters because of partial oxidation (fig. S15), but the alkenyl region resembled that of the PP-N $_2$ -wax.

As with the PE-derived waxes, upcycling of PP-N₂-wax and PP-air-wax was conducted in air

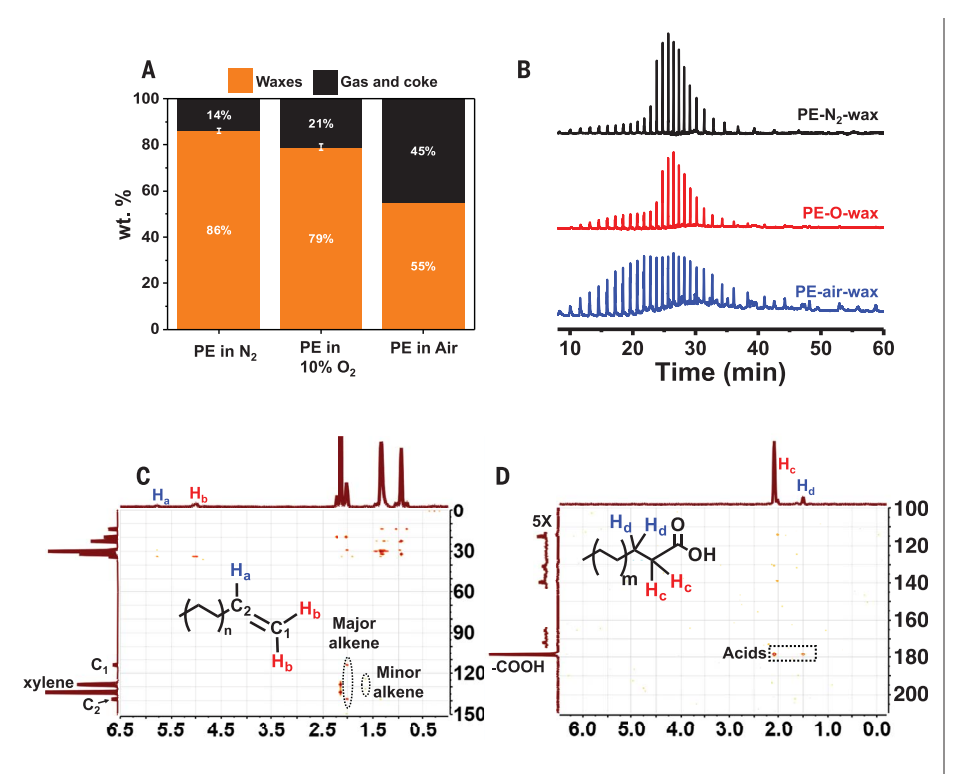


Fig. 2. Degradation of PE into intermediate waxes and upcycling into fatty acids. (A) Yields and (B) GC-MS chromatograms of intermediate waxes after degrading lab-grade PE in N_2 , 10 vol % of O_2 balanced with N_2 , or air. (C) NMR-HMBC spectra of PE- N_2 -wax in deuterated p-xylene. The circles highlight the C-H correlations of the major and minor alkene products. (D) NMR-HMBC spectrum of the fatty acid derived from PE-O-wax. The black box highlights the two carboxyl carbon correlations with protons. [Insets in (C) and (D)] Chemical structures of the major alkene and fatty acid products.

at 150°C over Mn stearate. PP-air-wax oxition was faster than that for PP-N2-wax; the former showed a CI of ~0.9 after 4 hours (fig. S9C). Moreover, a possible epoxy structure was detected in oxidized PP-air-wax (fig. S16), indicating that poxy could be a potential oxidation intermediate between alkenyl and aldehydes. The fatty acids (PP-air-FA) that resulted from hydrolysis were characterized by NMR-HMBC and showed no detectable aldehyde but stronger ketone carbonyl signals than those of PE-O-FA. The acid carbonyl showed three correlations with protons (Fig. 3C and fig. S17), possibly indicating a 2-carboxylpropyl terminal structure. PP-air-FA exhibited an AN of 169 mg KOH/g, substantially higher than the theoretical value of 84 mg KOH/g for a monocarboxylic acid at 670 g/mol (C46) (table S4, entry 6), suggesting the presence of polyacids.

After both PE and PP were successfully converted to wax and fatty acids at high conversions, municipal PE/PP wastes (obtained in Blacksburg, VA) were sorted (if labeled), pulverized, and mixed to mimic a waste stream [high-density PE (HDPE, 25 wt %), PP (25 wt %), low-density PE (LDPE, 25 wt %), and PE/PP unsorted (25 wt %)]. Three batches of the PE/PP waste

mixtures (500 mg per batch) were degraded into wax, resulting in an average yield of 82% in N_2 . The lower wax yield of PE/PP mixtures from municipal waste streams was ascribed to the additives, paint, dye, and labels. The wax was further upcycled to fatty acids, giving an average AN of 57.3 mg KOH/g (Fig. 1D and table S4, entry 8). The AN can be improved by tuning the oxygen level during degradation, the airflow during oxidation, and the upcycling temperature. Ketones and aldehydes could potentially be present in the product and can adjust the product viscosity, function as soap softeners (35), and modulate fragrance release (18).

Theoretical simulations

Density functional-based tight-binding (DFTB) simulations were used to gain a molecular understanding of the temperature-gradient degradation of PE and PP and to evaluate the subsequent oxidative upcycling reactions. DFTB and the extended tight-binding methods enable simulations of relatively large systems and reasonable timescales with good accuracy but are considerably faster than typical ab initio density functional theory (DFT) methods (36).

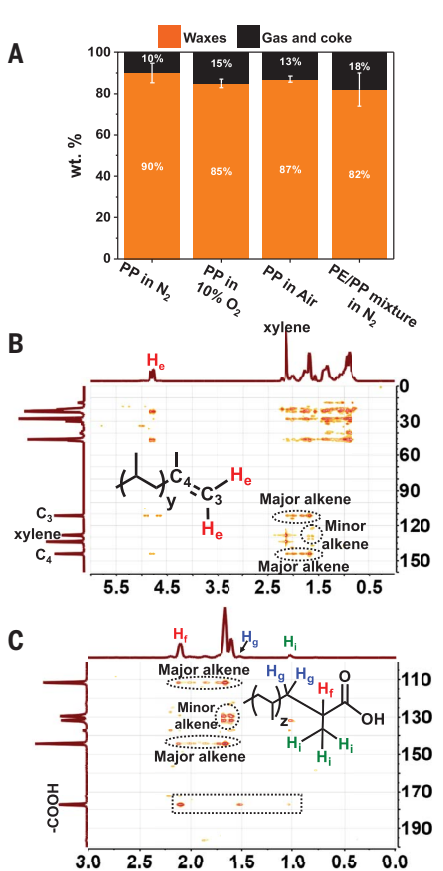


Fig. 3. Degradation of PP and PE/PP mixture into intermediate waxes and upcycling into fatty acids. (A) The intermediate wax yield of lab-grade PP upon degradation in N2, N2/O2 mixture (10 vol % O₂), or air, along with the wax yield from a PE/PP waste mixture (including 25 wt % HDPE, 25 wt % PP, 25 wt % LDPE, and 25 wt % PE/PP unsorted) upon degradation in N2. The ANs are shown in table S4. The low wax yield from the PE/PP waste mixture was due to solid contaminants such as paper labels, paints, and dyes. (B) NMR-HMBC spectra of PP-N₂-wax in deuterated p-xylene. (Inset) Chemical structure of the major alkene product. The circles highlight the C-H correlations of the major and minor alkene products, respectively. (C) NMR-HMBC spectra of PP-air-FA. (Inset) Chemical structure of the major fatty acid product. The black box highlights the three carboxyl carbon correlations with protons.

Multiple (>10) molecular-dynamics trajectories were used to evaluate the PP and PE chain behavior. The model polymer chains undergo significant coiling and dynamical oscillations during the ab initio molecular dynamics (AIMD) simulations. The mechanisms of alkene formation from PE and PP are primarily radical β -scission and secondarily disproportionation (Fig. 4A and fig. S18), similar to the findings of previous reports (3, 7, 38). We focus the discussion on PP because it produces more olefin wax

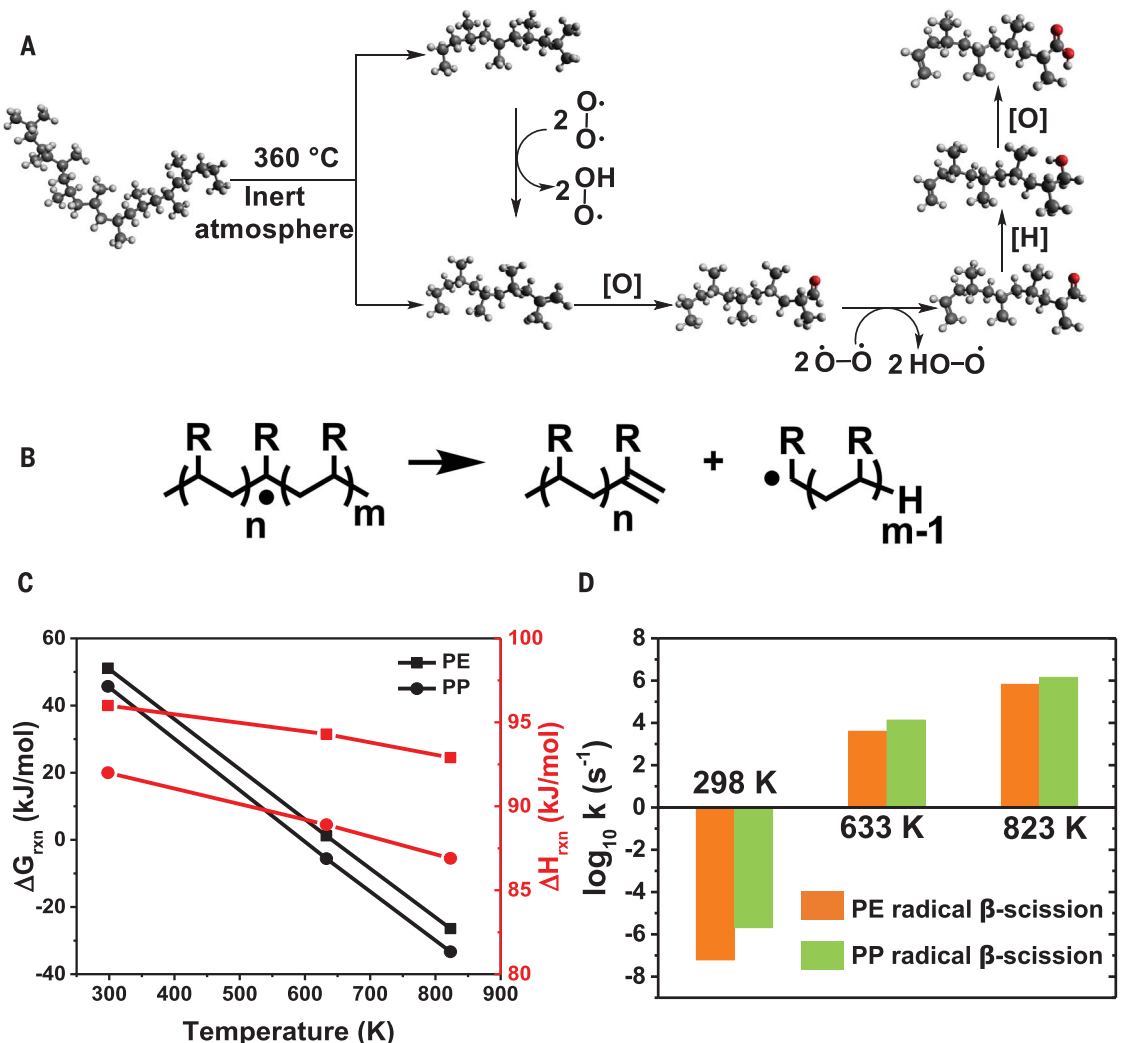


Fig. 4. Plausible reaction pathway, thermodynamics, and kinetics of **β-chain scission in PE** and PP. (A) The thermolysis of a model polymer chain into an alkane and alkene fragment and subsequent oxidation to a fatty acid, as captured by the simulations. (B) β-Scission of a radical in PE or PP. R=H or CH₃. (C) Thermodynamic parameters and (D) kinetic constants of PE B-scission and PP β-scission at 298, 633, and 823 K, as calculated according to the Benson group-additivity method (39, 40).

during degradation than does PE. The results show that chain scission occurs somewhat randomly along the backbone of the PP chain and that multiple bonds are broken to form alkene and alkane fragments (Fig. 4A and fig. S19). We note that the simulated fragment-size distributions agree with experimental observation and that there are more alkenes formed for PP than for PE. For example, in the experimental PE degradation, the initial C=C concentration in PE-N₂-wax was ~1.15 mmol/g on the basis of quantitative NMR (q-NMR, fig. S20 and table S5). By contrast, the C=C concentration in PP-N2-wax was ~3.15 mmol/g, showing good qualitative agreement with the simulation results.

The degradation fragments from the simulations were then annealed by geometry optimization and modeled for reactivity toward oxygen at reduced temperatures. During the oxidation step, hydrogen extraction from a methyl or methylene group in the fragment

was predicted to form a hydroperoxyl radical, which is prone to react with a readily formed aldehyde from alkenyl oxidation at the fragment end (Fig. 4A). This sequence initially produces an alcohol-like intermediate (H is transferred to carbonyl O on the aldehyde) that ultimately forms a carboxylic acid, by using a modified Baeyer-Villiger reaction. After the aldehyde accepts a H from the HOO., the O-O. binds to the intermediate C-OH to form a carboxylic acid. The aldehyde intermediate was confirmed by the NMR-HMBC experiments on partially oxidized wax (fig. S16). The primary intermediates found in this work also agree with the results of a previous study of paraffin oxidation over stearate (29), but we cannot rule out other potential oxidation pathways at this time.

Applying the qualitative insights from the DFTB simulations, we then used the Benson group-additivity method (39, 40) to evaluate the standard Gibbs free energy (ΔG°) (Fig. 4B and

table S6) of PE β -scission ($\Delta G_{PE}^{o} = 51.1 \text{ kJ/mol}$) and PP β -scission ($\Delta G_{PP}^{o} = 45.7 \text{ kJ/mol}$). Thermodynamically, alkene formation from PP and PE is disfavored at 298 K (Fig. 4C and table S7). At elevated temperatures (633 K and 823 K), PE β-scission and PP β-scission become increasingly thermodynamically favorable. Under our experimental conditions (633 K), the reaction enthalpies and ΔG° of PE and PP degradation are reduced ($\Delta H_{PP.633K}$ = 88.9 kJ/mol and $\Delta G_{PP.633K}$ = -5.60 kJ/mol; $\Delta H_{PE.633K} = 94.3 \text{ kJ/mol}$ and $\Delta G_{PE.633K}$ = 1.20 kJ/mol). However, the process is still slightly disfavored for PE. Upon increasing the temperature to 823 K, both PE and PP have favored β -scission pathways ($\Delta H_{\rm PP,823K}$ = 86.9 kJ/mol and $\Delta G_{PP.823K} = -33.1$ kJ/mol; $\Delta H_{\text{PE},823\text{K}}$ = 92.9 kJ/mol and $\Delta G_{\text{PE},823\text{K}}$ = -26.5 kJ/mol). The kinetic parameters and constants of β-scission were also predicted by using the group-additivity method on the basis of model reactions (fig. S21A) (41). PP β-scission showed lower activation energies and higher kinetic constants than did PE at all temperatures (Fig. 4D and table S8). In general, alkene formation from PP β -scission is more favored and faster than that from PE (this agrees well with our experiments and simulations above). Our observation of PE- and PP- β -scission dependence on temperature also agrees well with the literature, in which the alkene yield from PE thermolysis increased from ~30% at ~600 K to ~70% at above 800 K, whereas that from PP thermolysis stayed high (>70%) regardless of the temperature (fig. S22) (23, 37, 42–48).

Technoeconomic analysis (TEA) of the process was assessed on the basis of a 10,000-ton/year capacity (tables S9 to S14). The total capital investment was estimated at USD 2.70 million with an annual net profit of USD 1.03 million, resulting in an internal rate of return of 39.1%, a payback period of 2.63 years, and an average return of investment of 33.0%, without any government subsidies or tax returns (table S15).

Outlook

The fatty acids produced in this study have a wide range of applications, either for being kept in the plastic loop or for downstream uses. The downstream surfactant products have at least twice the market value of virgin plastics, representing an economically competitive process for plastic-waste utilization. In addition, surfactants have a market volume matching that of end-of-life plastic wastes, thus representing a volume-impactful method for plastic-waste removal. Controlled thermolysis in a temperaturegradient reactor is the key to controlling the high yield of the wax products relative to small gaseous molecules. Unlike existing processes (22), our process tolerates oxygen and requires no expensive catalysts or stringent reaction conditions. The resulting products show good ANs for PE- (96 mg KOH/g) and PP-derived fatty acids (169 mg KOH/g), which can be further optimized by inhibiting side reactions (figs. S23 and S24). We anticipate the process to be amenable to a diverse range of other plastic wastes for producing high-value, large-marketvolume products (e.g., fatty alcohols and sulfates) (49-51).

REFERENCES AND NOTES

- R. Geyer, J. R. Jambeck, K. L. Law, Sci. Adv. 3, e1700782 (2017).
- S. R. Nicholson, N. A. Rorrer, A. C. Carpenter, G. T. Beckham, Joule 5, 673–686 (2021).

- 3. J. Hopewell, R. Dvorak, E. Kosior, *Philos. Trans. R. Soc. Lond. Ser. B* **364**, 2115–2126 (2009).
- Y. Zhang, G. Wang, Q. Zhang, Y. Ji, H. Xu, Environ. Impact Assess. Rev. 93, 106728 (2022).
- B. A. Abel, R. L. Snyder, G. W. Coates, Science 373, 783–789 (2021).
- L. T. J. Korley, T. H. Epps III, B. A. Helms, A. J. Ryan, Science 373, 66–69 (2021).
- 7. C. Jehanno et al., Nature 603, 803-814 (2022)
- H. Chen, K. Wan, Y. Zhang, Y. Wang, ChemSusChem 14, 4123–4136 (2021).
 - Z. Huang et al., J. Am. Chem. Soc. 144, 6532-6542 (2022).
- 10. R. Cao et al., Nat. Commun. 13, 4809-4819 (2022).
- Z. Xu et al., Proc. Natl. Acad. Sci. U.S.A. 119, e2203346119 (2022).
 R. Conley, Ed., Thermal Stability of Polymers (Marcel Dekker, 1970).
- X. Jia, C. Qin, T. Friedberger, Z. Guan, Z. Huang, Sci. Adv. 2, e1501591 (2016).
- 14. F. Zhang et al., Science 370, 437-441 (2020).
- 15. W. Zhang et al., Science 379, 807-811 (2023).
- 16. R. J. Conk et al., Science 377, 1561-1566 (2022).
- 17. N. M. Wang et al., J. Am. Chem. Soc. 144, 18526-18531 2022).
- A. Trachsel, C. Chapuis, A. Herrmann, Flavour Fragrance J. 28, 280–293 (2013).
- 19. S. Kumar Sen, S. Raut, J. Environ. Chem. Eng. 3, 462-473 (2015).
- 20. L. R. Melby, Macromolecules 11, 50-56 (2002).
- 21. J. Y. Yao et al., Methods for the Decomposition of Contaminated Plastic Waste. US Patent US 11,220,586 B2 (2012).
- 22. U. Kanbur et al., Chem 7, 1347-1362 (2021).
- U. R. Gracida-Alvarez, M. K. Mitchell, J. C. Sacramento-Rivero, D. R. Shonnard, *Ind. Eng. Chem. Res.* 57, 1912–1923 (2018).
- A. Holmström, E. Sörvik, J. Appl. Polym. Sci. 18, 3153–3178 (1974).
- S. M. Al-Salem, A. Dutta, Ind. Eng. Chem. Res. 60, 8301–8309 (2021).
- 26. G. Celik et al., ACS Cent. Sci. 5, 1795-1803 (2019).
- V. Vrkoslav, R. Míková, J. Cvačka, J. Mass Spectrom. 44, 101–110 (2009).
- J. W. Frankenfeld, Ed., Study of Methods for Chemical Synthesis of Edible Fatty Acids and Lipids (NASA, 1968).
- P. George, E. K. Rideal, A. Robertson, *Proc. R. Soc. Lond. Ser. A* 185, 288–309 (1946).
- P. K. Roy, P. Surekha, R. Raman, C. Rajagopal, *Polym. Degrad. Stabil.* 94, 1033–1039 (2009).
- 31. F. Xiao, X. Sun, Z. Li, X. Li, ACS Omega 5, 12777–12788 (2020).
- 32. M. S. Stark, J. Am. Chem. Soc. 122, 4162-4170 (2000).
- 33. A. K. Pandey, R. K. Varshnaya, P. Banerjee, *Eur. J. Org. Chem.* **2017**, 1647–1656 (2017).
- 34. K. P. Sullivan et al., Science 378, 207-211 (2022).
- A. Meziani, D. Touraud, A. Zradba, M. Clausse, W. Kunz, J. Mol. Liq. 84, 301–311 (2000).
- 36. B. Hourahine et al., J. Chem. Phys. 152, 124101 (2020).
- H. Bockhorn, A. Hornung, U. Hornung, D. Schawaller, J. Anal. Appl. Pyrolysis 48, 93–109 (1999).
- 38. T. Kuroki, T. Sawaguchi, S. Niikuni, T. Ikemura, *Macromolecules* **15**, 1460–1464 (1982).
- S. W. Benson, J. H. Buss, J. Chem. Phys. 29, 546–572 (1958).
- R. L. Brown, S. E. Stein, in NIST Chemistry WebBook, NIST Standard Reference Database Number 69, P. J. Linstrom, W. G. Mallard, Eds. (National Institute of Standards and Technology, 2023); https://webbook.nist.gov/chemistry/.
- M. K. Sabbe, M. F. Reyniers, V. Van Speybroeck, M. Waroquier, G. B. Marin, ChemPhysChem 9, 124–140 (2008).
- A. Marcilla, M. I. Beltrán, R. Navarro, J. Anal. Appl. Pyrolysis 86, 14–21 (2009).
- D. Zhao, X. Wang, J. B. Miller, G. W. Huber, ChemSusChem 13, 1764–1774 (2020).
- J. K. Y. Kiang, P. C. Uden, J. C. W. Chien, *Polym. Degrad. Stabil.* 2, 113–127 (1980).

- M. T. S. P. De Amorim, C. Comel, P. Vermande, J. Anal. Appl. Pyrolysis 4, 73–81 (1982).
- 46. J. Michal, J. Mitera, S. Tardon, Fire Mater. 1, 160-168 (1976).
- G. Elordi, M. Olazar, G. Lopez, M. Artetxe, J. Bilbao, Ind. Eng. Chem. Res. 50, 6650–6659 (2011).
- 48. P. Das, P. Tiwari, Resour. Conserv. Recycling 128, 69-77 (2018).
- 49. H. Sabine, Oxidation of paraffinic hydrocarbons. US Patent US2391236A (1945).
- 50. D. V. Favis, Selective ozone oxidation of hydrocarbons. US Patent US2955123 (1956).
- 51. W. H. de Groot, Sulphonation Technology in the Detergent Industry (Springer, 1991).
- Z. Xu et al., Chemical upcycling of polyethylene, polypropylene, and mixtures to high-value surfactants, Dryad (2023); https://doi.org/10.5061/dryad.c866t1gc5.

ACKNOWLEDGMENTS

The authors acknowledge the Chemistry Chromatography Center at Virginia Tech, especially M. Ashraf-Khorassani, for providing GC and GC-MS support. The authors also acknowledge the Mass Spectrometry Incubator at Virginia Tech, especially R. Helm and K. Ray for their support on APCI-MS. The molecular simulations were performed at the Center for Nanophase Materials Sciences, a US Department of Energy (DOE) Office of Science User Facility operated at Oak Ridge National Laboratory. Funding: G.L. acknowledges support from the Department of Chemistry and the Dean's Discovery Fund at Virginia Tech. This material is partially based on the work supported by NSF Award DMR-1752611 through the CAREER award. Mechanistic studies of the deconstruction processes were partially supported by the US DOE Office of Science, Materials Sciences and Engineering Division. The simulations used resources of the Compute and Data Environment for Science (CADES) at the Oak Ridge National Laboratory, which is supported by the Office of Science of the US DOE under contract no. DE-AC05-000R22725. Funding for N.A.R. and J.M. was provided in part by the US DOE Office of Energy Efficiency and Renewable Energy, Advanced Manufacturing Office (AMO) and Bioenergy Technologies Office (BETO). This work was performed as part of the BOTTLE Consortium and was supported by AMO and BETO under contract no. DE-AC36-08G028308 with the National Renewable Energy Laboratory, operated by Alliance for Sustainable Energy, Author contributions: G.L. conceived and supervised the project. G.L. and Z.X. designed the project. Z.X. and N.E.M. conducted degradation-upcycling reactions and GC, GC-MS, and FTIR measurements. Z.X. and P.V. performed NMR experiments. B.G.S. conducted DFT simulations. Q.Z. performed TEA and heat and mass transfer analyses. N.E.M. and C.P. performed rheological experiments. N.R. and J.M. conducted HT-GPC measurements, 7.X. determined the standard Gibbs free energies for the degradation reactions. M.S. performed titrations to determine the ANs. N.E.M. evaluated the effect of temperature gradient on the degradation reactions. G.L., B.G.S., Z.X., and N.E.M. analyzed the data, interpreted the results, and wrote the manuscript. All authors proofread the manuscript. Competing interests: G.L., Z.X., and N.E.M. are inventors on Provisional Patent Application no. 63/462,863 pertaining to this work. Data and materials availability: Data pertaining to this work are available in the supplementary materials and Dryad (52). License information: Copyright © 2023 the authors, some rights reserved; exclusive licensee American Association for the Advancement of Science. No claim to original US government works, https://www.science.org/ about/science-licenses-journal-article-reuse

SUPPLEMENTARY MATERIALS

science.org/doi/10.1126/science.adh0993 Figs. S1 to S31 Tables S1 to S18 References (53–103)

Submitted 9 February 2023; accepted 16 June 2023 10.1126/science.adh0993

Xu et al., Science 381, 666-671 (2023) 11 August 2023 6 of 6